

Towards the Converged Von Neuman Peak Pressure using Fine Scale Simulation of Detonation Cell Structure

Jaehoon Ryu, Mohammed Niyasdeen and Jeong-Yeol Choi
Pusan National University
Busan, 46241, Korea

1 Introduction

All gaseous detonations are unstable and produce characteristic cell structure formed by the traces of triple points in the detonation wave-front and transverse shock wave behind the detonation wave. Detailed understanding of the physical and chemical process involved in the non-equilibrium structure of the detonation wave is essential to investigate detonation propagation mechanism and predict its dynamic parameters. Detonation wave-front instability has been studied since its first observation in 1961 [1]. Extended numerical studies have been conducted to investigate detonation wave structure [2-6], but only few studies focus on numerical requirements on detonation phenomenon.

In this study, a series of numerical simulations has been carried out to find a numerical requirement for capturing detonation cell structure efficiently. This fundamental investigation on detonation wave behavior will give an insight on numerical approach to investigation of detonation wave.

2 Numerical Methodology

2.1 Governing Equations

For a simplified modeling of detonation's dynamic process, a conservation of equation of reaction progress variable, Z , is introduced in addition to the conservation of mass, momentum and energy equations in two-dimensional coordinate as followed below.

$$\frac{\partial}{\partial t} \begin{bmatrix} \rho \\ \rho u \\ \rho v \\ \rho e \\ \rho Z \end{bmatrix} + \frac{\partial}{\partial x} \begin{bmatrix} \rho u \\ \rho u^2 + p \\ \rho uv \\ (\rho e + p)u \\ \rho uZ \end{bmatrix} + \frac{\partial}{\partial y} \begin{bmatrix} \rho v \\ \rho v^2 + p \\ (\rho e + p)v \\ \rho vZ \end{bmatrix} = \begin{bmatrix} 0 \\ 0 \\ 0 \\ 0 \\ \dot{\omega} \end{bmatrix} \quad \dot{\omega} = \rho(1 - Z) \cdot A \cdot \exp\left(\frac{-E_a}{p/\rho}\right)$$

$$p = (\gamma - 1) \cdot \rho \cdot \left\{ e - \frac{1}{2}(u^2 + v^2) + Zq \right\}$$

The reaction progress variable, Z , accounts for the mass fraction of product species which varies from 0 to 1 for unburned (reactant) to burned (product) state respectively. The chemical kinetics is modeled

by a 1-step irreversible Arrhenius reaction model. Where $\dot{\omega}$ is the mass rate of product formation, T_a is the activation temperature, and A is the pre-exponential factor. The pressure and temperature are obtained through the equations of state.

2.2 Numerical Methodology & Operating conditions

The governing equations are solved using a cell-vertex finite volume method. Roe, RoeM, AUSMDV, AUSMPW+ high order accuracy flux schemes are used for the convective fluxes in the cell boundaries [7-10]. As flux splitting schemes, 3rd-order MUSCL, 3rd-order WENO, 5th-order WENO and 5th-order oMLP schemes are used and compared each other [11-14]. The discretized equations are integrated in time using a 4th-order accurate 4-step Runge-Kutta scheme.

Moving computational window technique is applied to capture the important physics happening in the vicinity of the detonation wave-front. Incoming boundary is selected by checking the protruding detonation wavefront and the exit boundary is set to 1.5 times the channel width where characteristic boundary conditions is applied with C-J condition. One-dimensional steady ZND structure solution is used for initiation of detonation wave. A particular ZND condition are chosen in such way that a single detonation cell structure is obtained within the unit width channel.

3 Results

3.1 Grid Refinement

For the grid refinement tesst, straight channel with asepect ratio 100 with equal grid spacing in both x and y direction is used with various grid system as shown in table 1.

Table 1 Grid system configuration

Number of cells in unit channel width, n	Entire computational grid system	Size of moving computational window	Minimum spacing (Δy)
100	10,001 \times 101	151 \times 101	1/100
200	20,001 \times 201	301 \times 201	1/200
400	40,001 \times 401	601 \times 401	1/400
800	80,001 \times 801	1,201 \times 801	1/800
1,600	160,001 \times 1,601	2,401 \times 1,601	1/1600

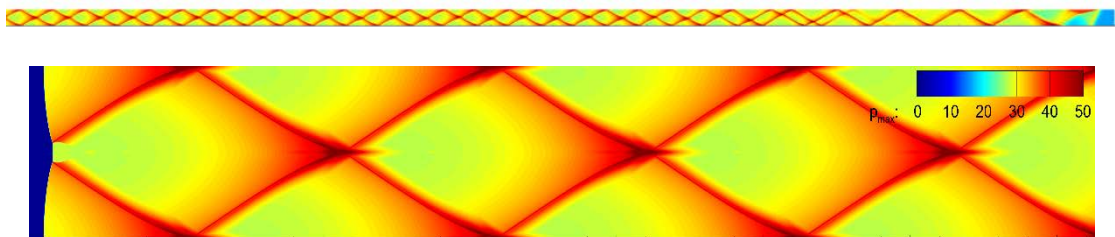


Figure 1: Entire numerical smoked-foil records for the channel of aspect ratio 100 (upper) and magnified plot of the detonation wave at the end of computation (lower)

Figure 2 shows the maximum pressure history at bottom wall for various grid resolutions. It is plotted in inverted direction for convenience. The averaged values of peak pressure and the cell length are plotted in figure 3. The averaged values are taken for the stabilized range $x/H = 50$ to 100 , because the early part is the transient period from the initial condition. Length of detonation cell is calculated by measuring the distance between two consecutive peak pressure points.

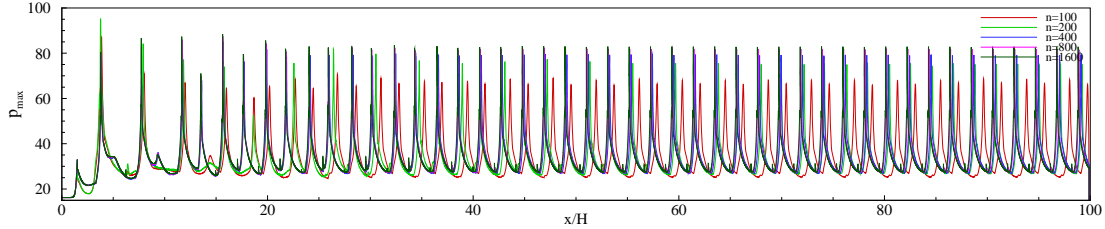


Figure 2: Maximum pressure history at bottom wall for various grid resolutions

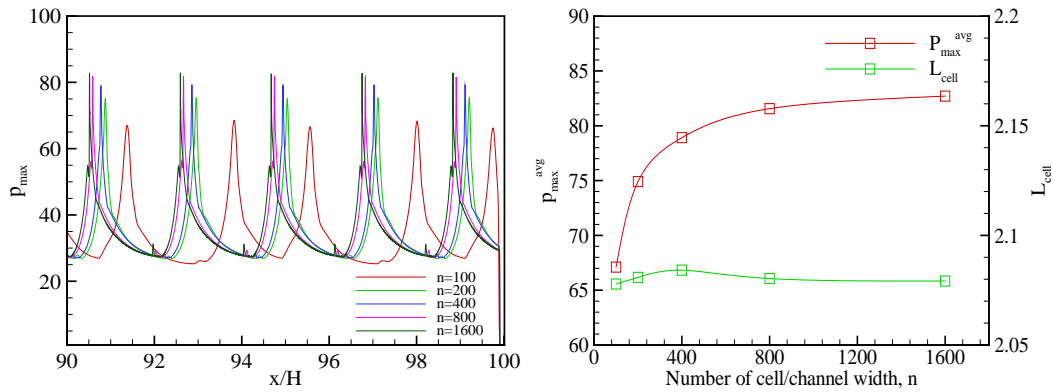


Figure 3: Close up view of Maximum pressure history at bottom wall for various grid resolutions (left) and averaged value of peak pressure and cell length for various grid resolutions (right)

The converging solution of the peak pressure and cell length along the grid resolution is shown on figure 3. It is found that variation of cell length is less affected by the grid resolution. Largest case is $n=400$, but the deviation is not so big. On the other hand, the average peak max pressure values converge as the number of grid points along the width increases. Both 800 and 1600 grid points along the width seems reasonably good enough to get a fine resolution. Present result implies that up 400 grid points along the width is needed to have converged value of Von Neumann peak pressure.

3.2 Dependency on Flux Schemes

Dependency test on high resolution schemes and flux splitting schemes has been conducted with $20,001 \times 201$ grid system. With RoeM flux splitting scheme fixed, 3rd-order MUSCL, 3rd-order WENO, 5th-order WENO, and 5th-order oMLP high resolution schemes analyzed. With MUSCL TVD scheme fixed, Roe, RoeM, AUSMDV, and AUSMPW+ flux splitting schemes have been investigated and compared. Maximum pressure and cell length are compared with each other and the finest resolution result for $n=1,600$. From figure 5, 5th-order WENO scheme shows the finest values among the high resolution schemes and RoeM scheme shows the finest solution among the flux splitting schemes.

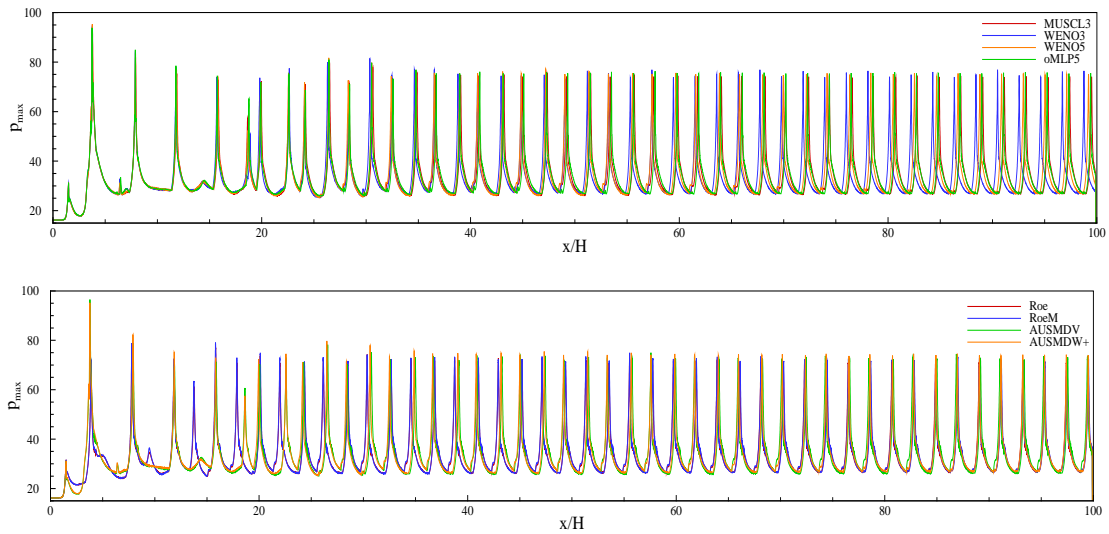


Figure 4: Maximum pressure history at bottom wall with different high-resolution schemes (upper) and maximum pressure history at bottom wall with different flux splitting schemes (lower)

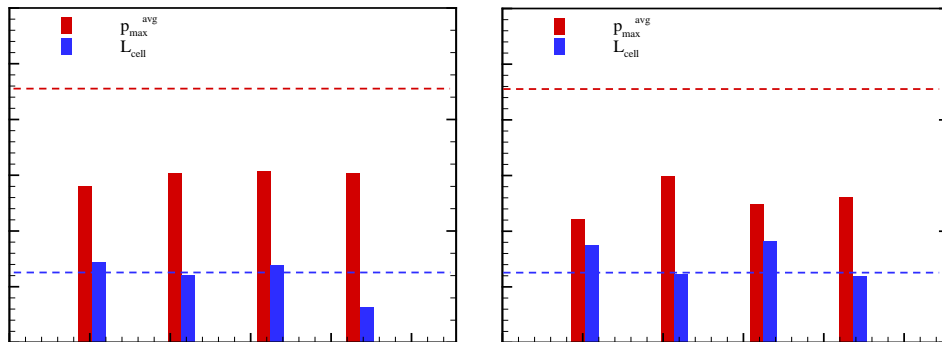


Figure 5: Averaged peak max pressure and cell length along high-resolution schemes (right) and flux splitting schemes (left)

3.3 Effect of Radius of Curvature

To investigate detonation wave propagation in a curved channel, additional numerical simulation has been conducted in two-dimensional circular channel with $R/H = 3.0, 4.5, 6.0,$ and 7.5 . 5th-order WENO and RoeM scheme with $10,001 \times 201$ grid resolution system is applied. Up $R/H=3.0$ cases satisfy the operating conditions of moving computational window, which assures detonation wave propagation. As shown on figure 7, inner and outer wall maximum pressure are different because of its geometrical characteristics. Outer wall is characterized by overdriven detonation, which is an accelerated condition than CJ condition and inner wall is underdriven detonation, deaccelerated condition than CJ condition. As the R/H increase, detonation wave propagation characteristic gets close to that of straight channel.

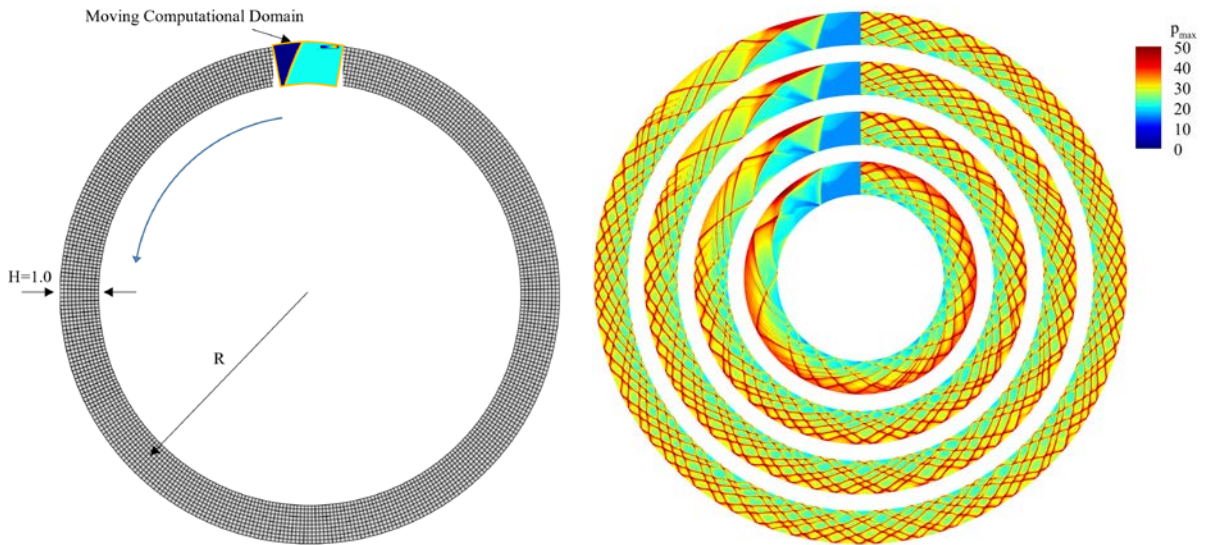


Figure 6: Coarse circular grid system with Moving computational domain (left) and numerical smoked-foil record of the circular channel of $R/H=3.0, 4.5, 6.0,$ and 7.5

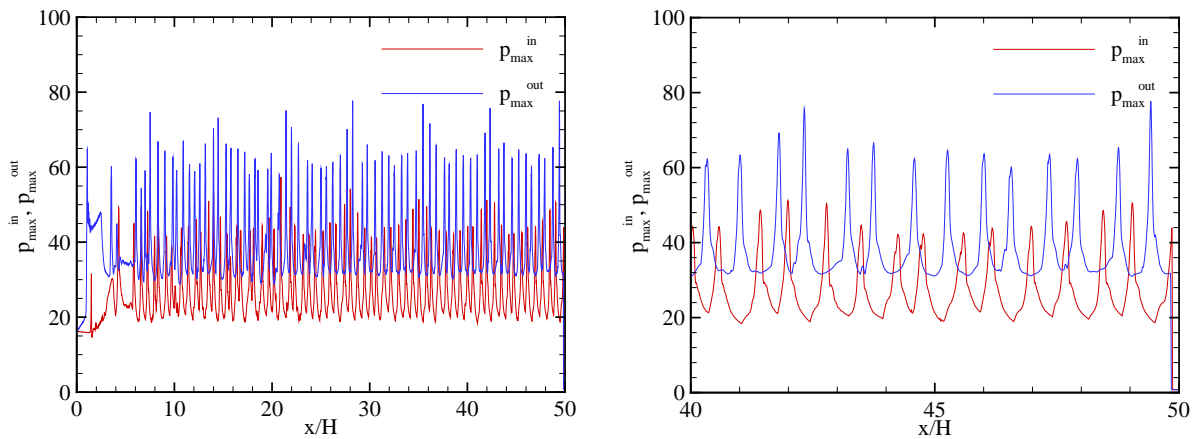


Figure 7. Entire maximum pressure history at inner and outer wall of $R/H=4.5$ circular channel (left) and close-up view of maximum pressure history at inner and outer wall (right)

4 Conclusion

Series of numerical investigation have been carried out to find out the numerical requirements for capturing fine detonation cell structure. Averaged peak max pressure and averaged cell length have been investigated for various grid resolutions, higher-resolution schemes and flux splitting schemes. Grid refinement study suggest that very fine resolution is required to have converged solution of Von Neumann peak pressure while the cell length is less affected by grid resolution. In the practical consideration, $n \geq 400$ provides the peak pressure 5% less than the converged solution. Investigating dependency on various numerical schemes suggests that 5th-order WENO flux scheme and RoeM flux splitting scheme provides the finest solution in the detonation cell structure study on straight channel. Detonation wave propagation in circular channel shows the overdriven and underdriven detonation characteristic at outer and inner walls to keep its propagation.

Acknowledgement

This work was supported by the Basic Science Research Program Grant (2019R1A2C1004505) through the National Research Foundation (NRF) of Korea, funded by the Ministry of Science and ICT (MSIT) of the Republic of Korea Government

References

- [1] White, D.R. (1961) Turbulent structure of gaseous detonation, *The Physics of Fluids*, 4(4):465-480.
- [2] Taki S, Fujiwara, T. (1978) Numerical analysis of two-dimensional nonsteady detonations. *AIAA Journal*, 16(1): 73-77.
- [3] Taki S, Fujiwara, T. (1981) Numerical simulation of triple shock behavior of gaseous detonation. In *Symposium (International) on Combustion*, 18(1):1671-1681
- [4] Kailasanath K, Oran ES, Boris JP, Young TR. (1985) Determination of detonation cell-size and the role of transverse-waves in two-dimensional detonations, *Combust. Flame*, 61(3):199–209
- [5] Choi JY, Jeung IS, Yoon Y. (2000) Computational fluid dynamics algorithms for unsteady shock-induced combustion. Part 1: Validation, *AIAA*, 38(7):1179-1187
- [6] Lee John HS. (2008) *Detonation phenomenon*. Cambridge University Press, doi.org/10.1017/CBO9780511754708
- [7] Roe PL. (1981) Approximate Riemann solvers, parameter vectors, and difference schemes. *Journal of computational physics*.43(2):357-72
- [8] Kim SS, Kim C, Rho OH, Hong SK. (2003) Cures for the shock instability: Development of a shock-stable Roe scheme. *Journal of Computational Physics*, 185(2):342-74.
- [9] Wada Y, Liou MS. (1997) An accurate and robust flux splitting scheme for shock and contact discontinuities. *SIAM Journal on Scientific Computing*, 18(3):633-57.
- [10] Kim KH, Kim C, Rho OH. (2001) Methods for the accurate computations of hypersonic flows: I. AUSMPW+ scheme. *Journal of computational physics*, 174(1):38-80.
- [11] Van Leer B. (1979) Towards the ultimate conservative difference scheme. V. A second-order sequel to Godunov's method. *Journal of computational Physics*, 32(1):101-36.
- [12] Jiang GS, Shu CW. (1996) Efficient implementation of weighted ENO schemes. *Journal of computational physics*, 126(1):202-28.
- [13] Henrick AK, Aslam TD, Powers JM. (2005) Mapped weighted essentially non-oscillatory schemes: achieving optimal order near critical points. *Journal of Computational Physics*, 207(2):542-67.
- [14] Kim S, Lee S, Kim KH. (2008) Wavenumber-extended high-order oscillation control finite volume schemes for multi-dimensional aeroacoustic computations. *Journal of Computational Physics*, 227(8):4089-122